An Experimental and Numerical Study of the Impact Response (V50) of Flexible Plain Weave Fabrics: Accounting for Statistical Distributions of Yarn Strength

7 AUTHORS, INCLUDING:

Ahmad A. Abu-Obaid
An-Najah National University
27 PUBLICATIONS **45** CITATIONS
SEE PROFILE

J. W. Gillespie Jr4
University of Delaware
464 PUBLICATIONS **5,359** CITATIONS
SEE PROFILE

Travis A. Bogetti
Army Research Laboratory
52 PUBLICATIONS **986** CITATIONS
SEE PROFILE

Rob Adkinson
Army Research Laboratory
6 PUBLICATIONS **31** CITATIONS
SEE PROFILE

An Experimental and Numerical Study of the Impact Response (V_{50}) of Flexible Plain Weave Fabrics: Accounting for Statistical Distributions of Yarn Strength

Gaurav Nilakantan [a,b], Cameron Showell [d], Ahmad Abu-Obaid [a], Michael Keefe [a,d], John W. Gillespie Jr. [a,b,c,*]

Travis A. Bogetti [e], Rob Adkinson [e]

[a] Center for Composite Materials
[b] Department of Materials Science and Engineering
[c] Department of Civil and Environmental Engineering
[d] Department of Mechanical Engineering
University of Delaware, DE 19716, USA

[e] US Army Research Laboratory
Aberdeen Proving Ground, MD 21005, USA

[*]Corresponding author. Tel.: +1(302)831-8149 (John W. Gillespie Jr.)
Email address: gillespi@udel.edu

ABSTRACT

Plain weave fabrics comprised of high-strength continuous-filament yarns such as Kevlar are used in many applications requiring impact and penetration resistance against high energy projectiles. Computationally simulating the impact of these fabrics using a finite element (FE) analysis is an extremely useful tool to investigate architectural and material effects on the performance of fabric systems. However for the past decade, many fabric FE models including both those with homogenized and explicit yarn level architectures often utilize a deterministic approach wherein all yarns in the fabric model are assigned to the same strength. However experimental studies show that the tensile strength distribution of yarns follows a statistical distribution, due to the inherent defects in each filament. This statistical variation in constituent yarn material properties is one of the major contributing factors to statistical variations in the performance of the fabric system under identical impact conditions. To enhance the predictive capability of the fabric FE model, it is important to be able to incorporate this statistical material data into the computational analysis. A series of impact simulations can then be run using a Monte Carlo approach. The scatter in residual velocity for a given impact velocity is tracked and compared to experimentally obtained results. This framework can then be applied to investigate the performance of fabrics comprised of different materials and architectures, as well as for different types of projectiles, leading to savings in the time and cost associated with the full scale experimental testing. The focus of this paper is to present the experimental data of statistical yarn strength, and the framework for incorporating this data into the FE model to statistically assess the fabric impact performance.

Gaurav Nilakantan, Center for Composite Materials, University of Delaware, DE, USA
Ahmad Abu-Obaid, Center for Composite Materials, University of Delaware, DE, USA
Cameron Showell, Department of Mechanical Engineering, University of Delaware, DE, USA
Michael Keefe, Department of Mechanical Engineering, University of Delaware, DE, USA
John W. Gillespie Jr., Center for Composite Materials, University of Delaware, DE, USA
Travis A. Bogetti, Army Research Laboratory, Aberdeen Proving Grounds, MD, USA
Rob Adkinson, Army Research Laboratory, Aberdeen Proving Grounds, MD, USA

1. INTRODUCTION

Materials such as Kevlar, Twaron, and Vectran have high strengths and tensile moduli making them desirable in applications that require impact and penetration resistance against high energy projectiles. These materials are often produced in the form of continuous filaments. These filaments are bundled together to form yarns that are further woven into 2D or 3D fabrics, or unidirectional tows that are further laid as plies in a resin impregnated composite structure. As seen from experimental quasistatic tensile testing of Leal et al. [1-2], the tensile strength of these filaments is not a single deterministic value; rather it is a set of values that can be well characterized by certain statistical distributions. Consequently the peak tensile strength of filament bundles or yarns also follows a statistical distribution. The predominant source of this variability is due to presence of inherent defects in the underlying structure. Secondary sources are the non-uniformity of filament diameter and cross-section along the length. Another interesting phenomenon is that this tensile strength is observed to decrease with increasing gage lengths due to greater probability of the presence of a critical defect or "weakest point" in the filament. At higher strain rates, these viscoelastic materials display an increase in the tensile stiffness and strength. The presence of twist in the yarns also affects the strength with the maximum strength often seen at a particular value of twist.

When fabrics comprised of these materials are used in flexible protective systems, there are three main energy absorbing and dissipating mechanisms that slow down the impacting projectile: (*i*) momentum transfer between projectile and fabric (*ii*) tensile elongation of yarns, and (*iii*) inter-yarn and projectile-fabric frictional sliding. The levels to which these mechanisms are active are broadly governed by three geometry parameters: yarn cross-section, yarn undulations, and fabric architecture; and four material parameters: tensile stiffness ($\boldsymbol{E}$), material density ($\boldsymbol{\rho}$), tensile strength ($\boldsymbol{\sigma_o}$), and coefficient of friction ($\boldsymbol{\mu}$). A high $\boldsymbol{E}$ to $\boldsymbol{\rho}$ ratio with a low $\boldsymbol{\rho}$ is desirable. This implies a system with low weight, low dynamic deflection, high stiffness, and a high longitudinal strain wave velocity. A faster wave velocity implies the local deformation and stresses are rapidly spread out to farther regions involving more fabric material in the energy absorption, which is desirable. Depending on the tightness of the weave, a moderate to high $\boldsymbol{\mu}$ is desirable. A very high value of $\boldsymbol{\mu}$, or more specifically the product of $\boldsymbol{\mu}$ and normal contact force, will tend to over constrain the sliding and reorientation of yarns leading to possible premature breakage. A very high σ_o is highly desirable as yarn breakage is severely detrimental to the impact performance of flexible fabrics. Of the four material properties, only $\boldsymbol{\sigma_o}$ is known to display a statistical distribution. Similar to $\boldsymbol{E}$, $\boldsymbol{\sigma_o}$ can also be strain rate dependent leading to changes in the shape of, and shifting in the location of, the statistical strength distributions used to characterize the data. Understanding the effect of the statistical nature of this material property on the overall impact performance is paramount in ensuring protective systems perform at certain levels, especially in human life-centric applications. For e.g. in human torso and extremity protection, knowing the V_0 velocity is critical, where $\boldsymbol{V_X}$ is defined as the velocity at which there is an X% probability of penetration. Thus V_0 is the velocity at which a striking impactor will be stopped by the protective system 100% of the time, correspondingly a 0% probability of penetration.

While filaments such as Kevlar initially possess high strengths (~3.2 GPa), the weaving processes that are employed to create the final woven fabric tend to degrade the tensile strength. Degradation mechanisms are primarily due to abrasion between the yarn and the loom elements, and between warp and weft yarns, which in turn are governed by the tension and velocity level settings employed. Large curvatures also induce compressive kink bands which may degrade tensile strength [3-4]. In certain materials, due to highly aligned rigid molecular chains, compressive straining is accounted for by kink band formation. This causes disruption of the alignment of the chains and possible void formation due to delamination, resulting in possible locations of crack initiation and stress concentrations, all leading to some loss in tensile strength. Other damage mechanisms associated with high strength materials such as Kevlar are due to broken primary and secondary bonds, for example separation of the radially pleated structure caused by failure of the already weak hydrogen bonds [1-2].

Figure (1) is a scanning electron microscope (SEM) image of filaments from a 600 denier Kevlar KM2 yarn which display some of the possible damage mechanisms in the filaments, as highlighted by the bold arrows. Compressive kink bands are observed along the filament length at more or less regular intervals. In addition, fibrillation is observed in one filament, where the skin structure shows signs of fibril peeling, leaving behind a groove on the surface. This is most probably caused by abrasion.

Since a larger σ_o is desirable, it is important to quantify the extent of weaving damages, its effect on the shape change and shift in the statistical strength distribution as well as its effect on the impact performance. There are other sources of strength degradation that could also be considered depending on their relative magnitude to weaving damages such as exposure to heat, moisture, and ultra violet radiation, ageing of the fabric, and manual handling and re-spooling of the yarns and fabrics.

The first step in this research is to generate the experimental yarn tensile

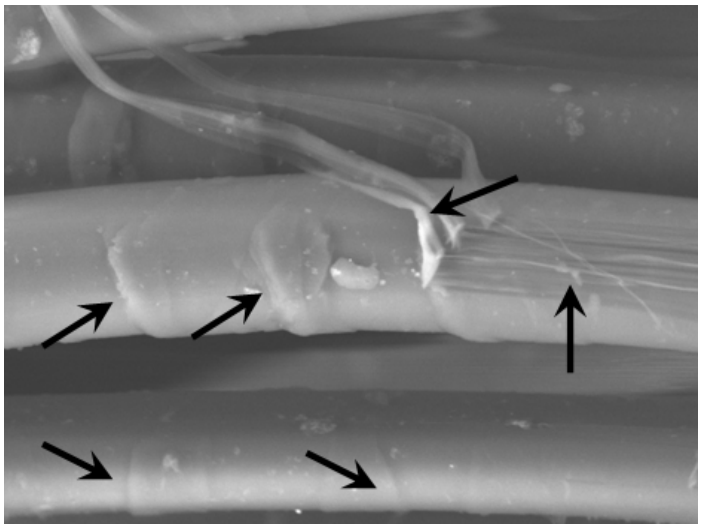

Figure 1. SEM image of damaged filaments from a 600 denier Kevlar KM2 yarn

strength data and apply statistical techniques to characterize this data. Next, the overall framework from setting up the fabric model finite element mesh using micrographs to mapping the experimental data onto the FE mesh needs to be set up. These steps form the focus of this paper. Afterwards, experimental fabric impact testing and Monte Carlo simulations need to be conducted and results compared to validate the methodology. This will ultimately yield a reliable and predictive computational framework that will reduce the dependency on full scale experimental testing to statistically evaluate the impact performance of flexible fabrics used in protective applications.

2. EXPERIMENTAL TENSILE TESTING OF YARNS

To develop the experimental tensile strength data set, three sources of continuous filament yarns were selected. The first source comprised of 600 denier Kevlar KM2 yarns extracted from a spool. The second and third sources respectively comprised of warp and fill yarns carefully extracted from greige and scoured Kevlar S706 fabrics. The Kevlar yarn was manufactured by DuPont while the fabric was woven by the Hexcel Corporation. All materials were received in an "as-is" condition from the Army Research Lab (ARL), Aberdeen Proving Grounds, MD, USA. These continuous filament Kevlar KM2 yarns have very little twist and comprise of 400 filaments of approximately 12 micron diameter with a density of 1.44 g/cm^3. The Kevlar S706 fabric is a plain weave fabric comprised of these 600 denier Kevlar KM2 yarns, with a count of 34 yarns per inch in the warp and fill directions, and an areal density of 180 g/m^2. Greige fabric refers to the woven fabric fresh off the loom while scoured fabric refers to a greige fabric that has been repeatedly mechanically washed in a hot solution. Scouring is done to remove any foreign particles and broken monofilaments from the fabric as well as to change or improve the surface behavior of the fabrics making them amenable to further surface treatments. The yarns from the spool form the control samples from which yarns later extracted from the fabrics will be compared against to assess weaving damages. Yarn samples of gage lengths varying between 1 in. and 15 in. were prepared from all three sources and then end-tabbed using thin one inch cardboard squares. Before testing, all end-tabbed specimens were placed for a minimum of 15 hours in a vacuum oven maintained at room temperature. An Instron Model 5567 with a ±500 N load cell, see Figure (2), was used for testing. In accordance with ASTM standard D7269-07 "Standard Test Methods for Tensile Testing of Aramid Yarns", the cross head speed for the quasi static tensile testing in inches/min was set at 50% of the gage length in inches, which corresponds to a strain rate of 0.5 min^{-1}. This is important to ensure strain rate effects are not included in the data when comparing samples of different gage lengths. The recorded data of interest were the maximum load (N) and tenacity at maximum load (g/den). For convenience, the tenacity data in units of *g/den* is also converted into strength data in units of *MPa*. A minimum of 30 data points are required for the statistical analysis in order to achieve a good fit the data points, and correspondingly most tests were conducted till at least 50-90 data points were generated. The yarns were not preconditioned at elevated temperatures, and no twist was imparted. End tabbing was preferred over using Bollard type jaws since the gage lengths could be

Figure 2. (a) Instron Model 5567 (b) Load cell and grips

accurately assessed which was important for studying length scale effects, also the minimum gage length possible with the jaws was limited to around 6 in., however specimens as small as 1 in. could be prepared with end-tabbing.

3. REVIEW OF THE STATISTICAL ANALYSIS TECHNIQUES

After recording the tenacity-at-maximum-load data for all samples at each gage length from all three sources, each series data is arranged in an increasing order of magnitude and then median ranks (MR) are assigned to each tenacity data point. Each median rank yields the cumulative probability of failure at that particular tenacity. It is given by

$$MR = \frac{i - 0.3}{N + 0.4} \tag{1}$$

where ***i*** is the sample number and ***N*** is the sample size. Next, statistical distributions are selected to fit the MR data. Some of the most common distributions used in survivability studies, particularly for characterizing filament, yarn, and tow strength data are the Weibull and to a lesser extent, the Gumbel distributions [1, 3-7, 9-10]. Based on a comparative analysis of the correlation coefficient and goodness of fit of over ten statistical distributions using the software Reliasoft Weibull++® [8], two distributions were selected that consistently provided the best fit of the experimental data. They were the G-Gamma (*G=Generalized*) and 3-parameter Weibull distributions. The following is a review of some of the useful mathematical

formulae used in the statistical analyses, from Ref. [8]. The probability density function (PDF) of the G-Gamma distribution is given by

$$f(t)=\frac{\beta}{\Gamma(k)\theta}\left(\frac{t}{\theta}\right)^{k\beta-1}\exp\left(-\left(\frac{t}{\beta}\right)^{\beta}\right) \tag{2}$$

where $\theta>0$ is the scale parameter, $\beta>0$ and $k>0$ are the shape parameters, and $\Gamma(x)$ is the gamma function of x. Here t is the variable which represents the tenacity at maximum load (g/den) or strength (MPa). The problem associated with this form of the PDF is that even with 200 or more data points, the Maximum Likelihood Estimator (MLE) methods fail to converge and some distributions with widely varying scale and shape parameters appear almost identical. The software Weibull++® uses a reparameterization with parameters μ, σ, and λ where

$$\mu=\ln(\theta)+\frac{1}{\beta}\ln\left(\frac{1}{\lambda^2}\right) \qquad \sigma=\frac{1}{\beta\sqrt{k}} \qquad \lambda=\frac{1}{\sqrt{k}} \tag{3}$$

The PDF can now be represented as

$$f(t)=\frac{|\lambda|}{\sigma t}\cdot\frac{1}{\Gamma\left(\frac{1}{\lambda^2}\right)}\cdot e^{\left[\frac{\lambda\frac{\ln(t)-\mu}{\sigma}+\ln\left(\frac{1}{\lambda^2}\right)-e^{\lambda\frac{\ln(t)-\mu}{\sigma}}}{\lambda^2}\right]} \quad \text{if } \lambda\neq 0 \tag{4a}$$

$$f(t)=\frac{1}{t\sigma\sqrt{2\pi}}\cdot e^{-\frac{1}{2}\left(\frac{\ln(t)-\mu}{\sigma}\right)^2} \quad \text{if } \lambda=0 \tag{4b}$$

The cumulative distribution function (CDF), which will be used to obtain the cumulative probability of failure at a particular tenacity or strength, is given by

$$F(t)=\Gamma_I\left(\frac{e^{\lambda\left(\frac{\ln(t)-\mu}{\sigma}\right)}}{\lambda^2};\frac{1}{\lambda^2}\right) \quad \text{if } \lambda>0 \tag{5a}$$

$$F(t)=1-\Gamma_I\left(\frac{e^{\lambda\left(\frac{\ln(t)-\mu}{\sigma}\right)}}{\lambda^2};\frac{1}{\lambda^2}\right) \quad \text{if } \lambda<0 \tag{5b}$$

where $\Gamma_I(k;x)$ is the incomplete gamma function of k and x.

Although many studies in the literature use the Weibull distribution to characterize the data, the G-Gamma distribution has also been used here as it is

more flexible and often provides a better fit. In fact the Weibull distribution is a special case of the G-Gamma distribution when λ=1, β=1/σ, and η=ln(μ).

There are three commonly used forms of the Weibull distribution: 2-parameter, 3-parameter, and bi-modal. In this study, the 3-parameter Weibull distribution was chosen over the other two as it consistently gave a better fit. The PDF of the 3-parameter Weibull distribution is given as

$$f(\sigma) = \left(\frac{m}{\sigma_0}\right)\left(\frac{(\sigma - x)}{\sigma_0}\right)^{m-1} \exp\left(-\left(\frac{(\sigma - x)}{\sigma_0}\right)^{m}\right) \tag{6}$$

and the CDF is given as

$$F(\sigma) = 1 - \exp\left(-\left(\frac{(\sigma - x)}{\sigma_0}\right)^{m}\right) \tag{7}$$

where σ_0 is the scale parameter, m is the shape parameter, and x is the threshold parameter. The 3-parameter Weibull is usually used when the MR data points do not lie on a straight line when plotted on Weibull probability paper, and display some concavity or convexity. Then x is a number which is subtracted from the MR data points in an attempt to make the shifted coordinates fall on a straight line. In such as case, the parameter x has physical significance, of being the maximum strength below which there is no yarn failure, i.e. the first instant of failure occurs at a value greater than x. However this is not always the case, especially when x is a negative number, and sometimes the 3-parameter Weibull distribution is chosen as it simply provides a better fit than the 2-parameter Weibull distribution. In the case of the 2-parameter Weibull distribution, x=0.

The correlation coefficient is often used to decide upon the choice of distribution that is employed to fit the MR data, between the G-Gamma and Weibull distributions. Sometimes the two correlation coefficients are almost identical in magnitude. In such as case, a visual inspection is made of the plots to see which distribution better fits the data especially around the head and tail ends of the CDF distribution, and this is left to the discretion of the analyst.

4. RESULTS AND DISCUSSION OF EXPERIMENTAL TENSILE TESTING

Figure (3) displays the CDF and PDF distributions of the 4 inch gage length samples from all three yarn sources, while Figure (4) displays the same data for the 15 inch gage length samples. Due to limited available space, the results of only two gage lengths have been presented here. Table (I) lists the statistical distribution parameters used to characterize the experimental data in Figures (3) and (4). The list of symbols are as follows: spool (*S*), greige fabric warp yarn (*GW*), greige fabric fill yarn (*GF*), scoured fabric warp yarn (*SW*), scoured fabric fill yarn (*SF*), G-Gamma distribution (*GG*), 3-parameter Weibull distribution (*3P*), and correlation coefficient (ρ). The three parameters (*P1-P3*) respectively represent: μ, σ, and λ (for

the G-Gamma distribution) and m, σ_0, and x (for the 3-parameter Weibull distribution).

Table I. List of statistical distribution parameters used to characterize the experimental data

Source	*GL (in.)*	*Type*	*P1*	*P2*	*P3*	*ρ*
S	4	GG	7.9739	0.0324	0.8578	0.9976
GW	4	3P	10.3268	556.9807	1885.732	0.9910
GF	4	3P	1.8751	163.9135	2504.7721	0.9832
SW	4	3P	15.1862	611.7679	1462.4008	0.9970
SF	4	3P	2.3359	185.972	2391.1297	0.9889
S	15	3P	2.3666	205.7002	2528.2644	0.9857
GW	15	3P	6.85	342.6437	1830.07	0.9918
GF	15	3P	56.5784	3308.95	-781.5434	0.9814
SW	15	3P	2.0296	96.6988	1801.8559	0.9979
SF	15	3P	2.0323	69.557	2272.34	0.9885

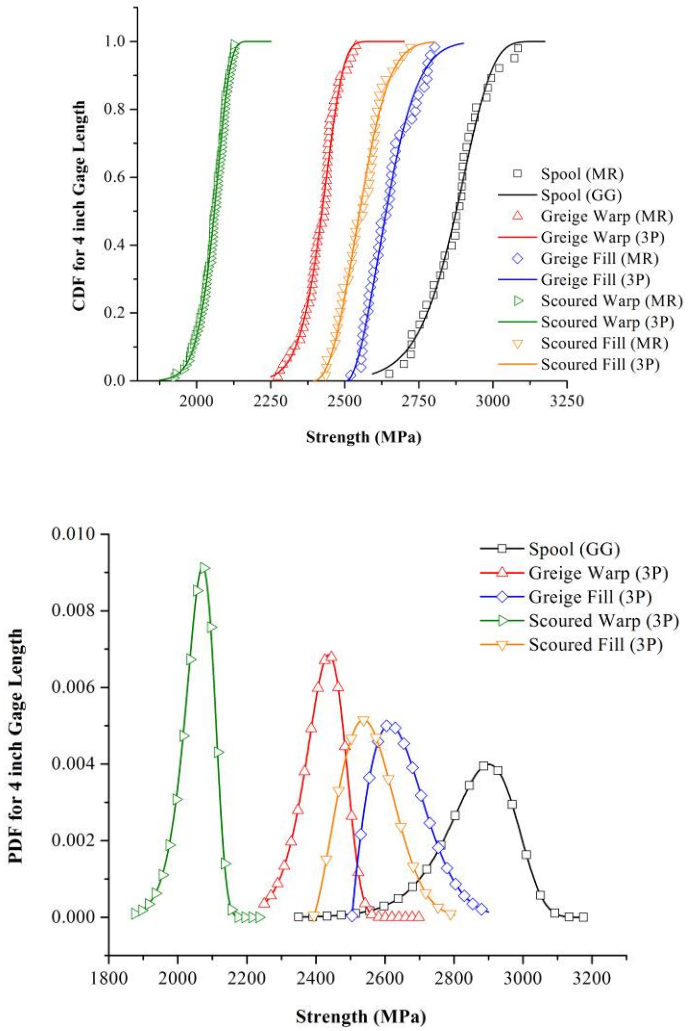

Figure 3. Probability distributions for 4 inch gage length 600 denier Kevlar KM2 yarn specimens (top) CDF (bottom) PDF

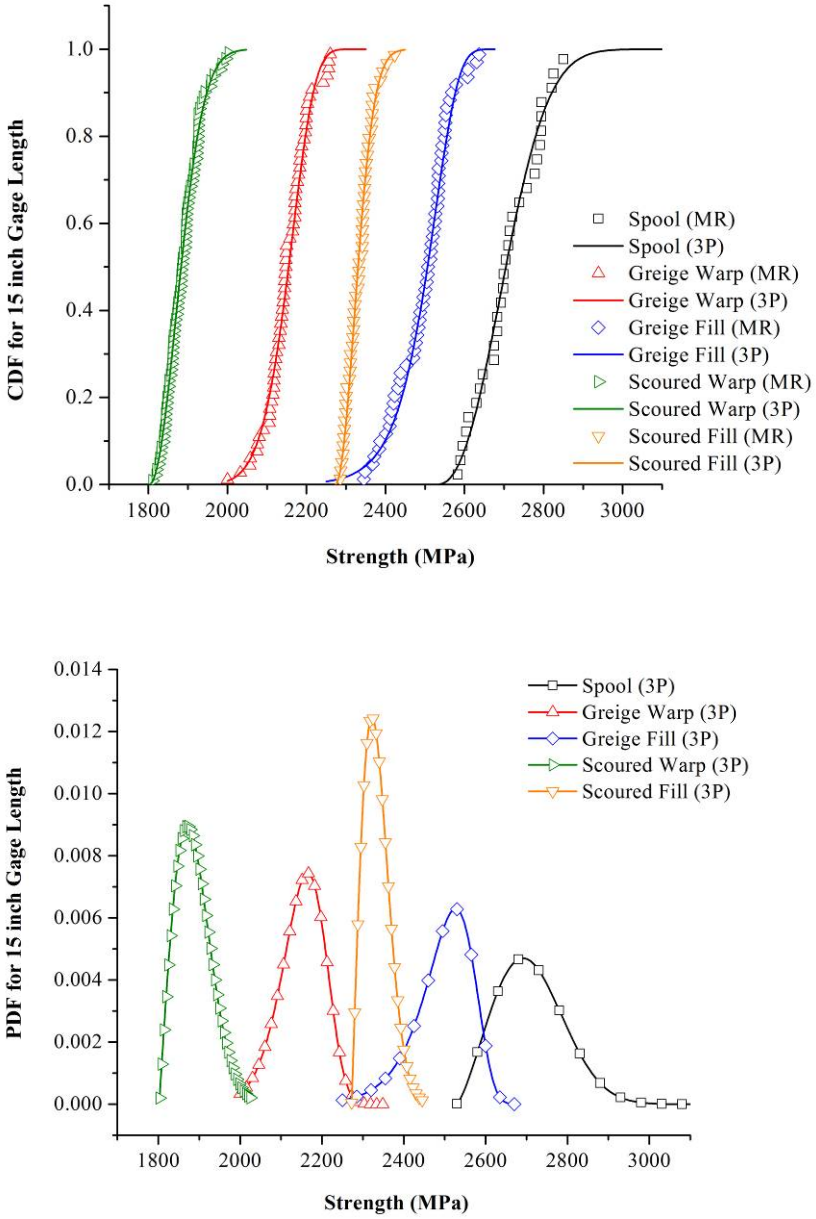

Figure 4. Probability distributions for 15 inch gage length 600 denier Kevlar KM2 yarn specimens (top) CDF (bottom) PDF

As seen from Figures (3) and (4), the strength of yarns extracted from the fabrics are lower than the spool which formed the control sample. This indicates that weaving damages are present, which tend to shift the CDF distributions of the extracted yarns to the left, or to lower strengths. The strength of warp yarns is always lower than the strength of the fill yarns, or the warp yarn CDF distributions lie to the left of the fill yarn CDF distributions. This implies that the warp yarns undergo more weaving strength degradations than the fill yarns. Also the strength

of the warp (and fill) yarns extracted from the scoured fabric are lower than the strength of the warp (and fill) yarns from the greige fabric, indicating that the scouring process also degrades strength. Upon comparing Figures (3) and (4) with the corresponding plots of the 1 in., 2 in, and 10 in. gage length specimens which are not shown here, the degradation of the scoured warp yarn when compared with the greige warp yarn is greater than the degradation of the scoured fill yarn when compared with the greige fill yarn. Further the extent of this degradation is gage length dependent with smaller gage length showing larger degradations between the yarns from the greige and scoured fabrics.

In order to quantify the extent of weaving damages, the strength retention factor (*SRF*) is used, which is given as

$$SRF_{\mathrm{X}} = \left. \frac{\text{Sample Strength}}{\text{Control Sample Strength}} \right|_{\text{at X\% cumulative probability of failure}} \tag{8}$$

Table (II) lists the strength retentions of the 4 inch gage length yarn samples extracted from the greige and scoured fabrics, with all values normalized with respect to the samples from the spool, viz. control samples. The strength retentions have been calculated at 10%, 50%, and 90% cumulative probabilities of failure. Table (III) lists similar information for the 15 inch gage length samples.

Another noticeable trend upon comparing the data from Tables (2) and (3) as well the corresponding data of the other gage lengths not shown here is that the strength retention decreases with increasing gage lengths when comparing the same yarn source at the same cumulative probability of failure. Thus the weaving damages also exhibit some form of length scale effects, in addition to the inherent length scale effect of the strength of the control sample at varying gage lengths. As mentioned earlier, the length scale effect is due to the increased probability of a critical defect with increasing gage lengths. This drives the CDF distributions to lower strengths or to the left at increasing gage lengths. To illustrate this effect, the median ranks assigned to the strengths at varying gage lengths of the control sample

Table II. Strength retention of 4 inch gage length 600 denier Kevlar KM2 yarn samples

4 in. Gage Length	**Retention at X% cumulative probability of failure**		
	10%	**50%**	**90%**
Spool	1.00	1.00	1.00
Warp, Greige	0.85	0.84	0.82
Fill, Greige	0.94	0.92	0.92
Warp, Scoured	0.73	0.72	0.70
Fill, Scoured	0.90	0.89	0.88

Table III. Strength retention of 15 inch gage length 600 denier Kevlar KM2 yarn samples

15 in. Gage Length	**Retention at X% cumulative probability of failure**		
	10%	**50%**	**90%**
Spool	1.00	1.00	1.00
Warp, Greige	0.80	0.80	0.79
Fill, Greige	0.91	0.93	0.91
Warp, Scoured	0.70	0.70	0.69
Fill, Scoured	0.88	0.86	0.84

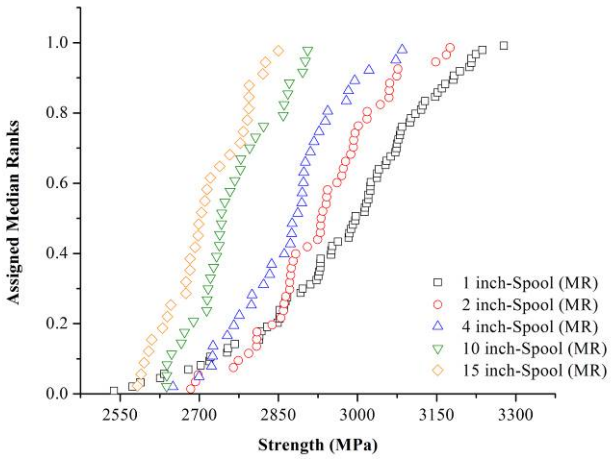

Figure 5. Length scale effects in the strength of the 600 denier Kevlar KM2 yarns from the spool

have been plotted in Figure (5).

It is also evident that the CDF plots become steeper at increasing gage lengths. This implies the scatter in strengths becomes smaller and clusters closer together around a lower value. Correspondingly, the PDF plots would become narrower and shift to the left at increasing gage lengths.

Length scale effects are an important consideration during the simulation of the fabric impact event. Only the yarn material behind the front of the longitudinal strain wave participates in the tensile deformation and energy absorption, while the material ahead of the wave front has no information of the arriving wave. When assigning strengths to the yarns in the FE model, the location of the front of the wave needs to be tracked so that the yarn strength can accordingly be adjusted depending on the length of yarn involved. This applies to the cases of very high impact velocities where there is a possibility of failure before the longitudinal wave reaches the fabric boundaries. However for lower impact velocities, rather than tracking the location of the front of the wave, the fabric in-plane dimensions of length and width could be used to accordingly scale the strength of the yarns, since once the wave front reaches the boundaries the entire yarn length will be involved in the impact event. Whichever the case may be, it becomes apparent that it is not feasible to conduct experimental testing at every possible gage length since it is a laborious and time consuming process. Rather, a technique is needed to be able to extrapolate the CDF plots to any gage length using the known data of a single gage length.

To account for the gage length effect, many researchers, for example Refs. [5-7, 9], use the factor (***L***/***Lo***) in Equation (7), where ***L*** refers to the current gage length (or length to which the data needs to be extrapolated) and ***Lo*** refers to the original gage length (or length at which the testing the experimental testing was conducted). Thus Equation (7) becomes

$$F(\sigma) = 1 - \exp\left(-\left(\frac{L}{L_0} \right) \left(\frac{(\sigma - x)}{\sigma_0} \right)^m \right) \tag{9}$$

Since Equation (9) does not consistently work well with all types of fibers, and sometimes overestimates the strength of fibers with length $L<Lo$ and underestimates for $L>Lo$, Wu and Netravali [9] report on the modification made to Equation (9) wherein a factor α is introduced so that the length scaling equation now becomes

$$F(\sigma) = 1 - \exp\left(-\left(\frac{L}{L_0} \right)^{\alpha} \left(\frac{(\sigma - x)}{\sigma_0} \right)^{m} \right) \tag{10}$$

Here α ranges between 0 and 1. Phoenix et al. [10] have computed an α value of 0.6 for Kevlar 49 fibers. One reason postulated for the introduction of the factor α is that the diameter of filaments varies within the yarn cross section. However since the diameter of a filament also varies along the filament length, the applicability of Equation (10) is limited to range around the length Lo [9].

In attempting to use Equation (9) to fit the data in Figure (5), we find that Equation (9) also tends to over and under estimate the strengths. However we also found that using a single value for α in Equation (10) did not consistently work either. Hence we postulate a new form for α as follows, where

$$\begin{aligned} &\alpha = \alpha_1 \text{ for } L < Lo \\ &\alpha = \alpha_2 \text{ for } L > Lo \\ &\alpha = 1 \text{ for } L = Lo \end{aligned} \tag{11}$$

Following Equation (11), and using α=0.8 for $L<Lo$ and α=1.6 for $L>Lo$, the strength data reported in Figure (5) are fit using the modified length scaled 3-parameter Weibull distributions as shown in Figure (6). The CDF of the 4 inch gage length yarn samples from the spool are used to extrapolate the CDFs of the other gage lengths viz. 1 in., 2 in., 10 in., and 15 in. also extracted from the spool. As can be seen from Figure (6), a very good fit of the MR data is achieved. This procedure was repeated on the other gage lengths as well, not shown here. Such a formulation would prove extremely useful during the assigning of tensile strengths to the yarns in the FE model of the woven fabric, where experimental testing using a few gage lengths could be extrapolated over a wide range of gage lengths; that could pertain to either the in-plane dimensions of the fabric or the instantaneous distance travelled by the longitudinal wave front from the point of impact, that determines the length of yarn involved in the deformation and stress buildup.

5. EXPERIMENTAL IMPACT TESTING OF FABRICS

In order to assess the applicability of this framework to computationally assessing the statistical impact performance of fabrics, simulation results need to be compared with experimental results. However due to uncertainties associated with experimental testing, there are important points to consider while making these comparisons, and some of these will be outlined in this section.

Over the past few decades, standards have been created to set minimum performance requirements and establish a set of test methods for the impact resistance of personnel protective clothing. One example is the U.S. National Institute of Justice *NIJ-Standard-0101.06*. Another example is the U.S. Army standard *MIL-STD-662F* which provides guidelines to determine the V_{50} limit of protective systems. The NIJ standard requires the use of backing materials such as clay which are meant to model the human torso response. Large back-face deformations of the personnel protective systems under impact can cause blunt force trauma injuries that are potentially life threatening. Accordingly the NIJ standard sets a maximum back-face deformation depth of 44 mm. As mentioned earlier, computational modeling allows for an in-depth investigation of the basic fundamentals of the impact physics, deformations, and energy absorbing mechanisms. With the advent of numerical codes such as LS-DYNA and high speed computing infrastructure, the use of techniques such as the finite element analyses (FEA) have become very popular. However computational modeling of this backing material proves very challenging for two reasons. One is the tremendous computational expense required to run impact simulations with the presence of the backing material, since a fine mesh is required whose element size corresponds to that used to discretize the yarns in order for the contact algorithms between the fabric and clay to function properly without large interpenetrations. The second is the complex material behavior of the clay that is temperature dependent, visco-elastic, exhibits flow, and is difficult to experimentally characterize. Therefore computational material modeling of the backing material response is difficult and requires further investigation since information is scarcely available in the literature. Further the depth of information that can be obtained from an experimental test with backing material is quite restricted, and is often only the final deformed shape of the clay and the depth of deformation. As a result, it is useful to conduct experimental impact testing of fabrics without any backing materials. Grips and frames are used to hold the fabric target in place. This allows

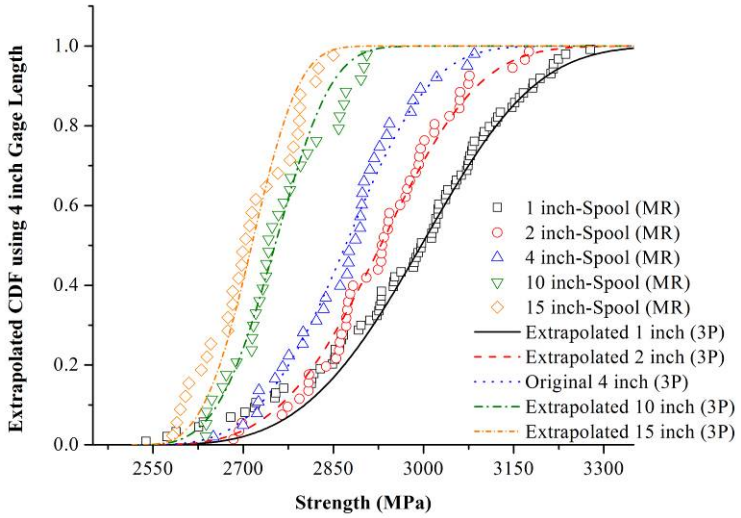

Figure 6. Extrapolated CDFs using the 4 inch gage length 600 denier Kevlar KM2 yarn from the spool

the setting up of high speed video cameras around the fabric and the use of techniques such as Digital Image Correlation (DIC) to record the deformations, interactions, and projectile velocity in real time. Changing the type of clamping or fabric boundary condition drastically influences the dominant mode of energy absorption and deformation. Clamping a fabric on four sides creates a yarn tension and elongation dominated mode of deformation while clamping a fabric at the four corners creates a yarn reorientation and frictional sliding dominated initial mode of deformation. Clamping a fabric on two sides produces a mixture of the above two mechanisms. Similarly, clamping the fabric either with the warp and fill yarns perpendicular to the grips (normal mode with 0°-90°) or inclined (bias mode with ±45°) also affects the dominant mode of energy absorption. Thus by suitably varying the boundary conditions and fabric orientation, the contribution of each type of energy absorbing mechanism for a given fabric architecture and material could be studied in order to optimize the impact performance. However this method is not without its own limitations, primarily slippage of the fabric from underneath the grips since perfect clamping of flexible fabrics is very difficult. Figure (7) displays some examples of clamped Kevlar S706 fabrics after impact that have been completely penetrated by 0.22 caliber smooth steel ball bearing projectiles. The first case consists of multiple layers of a bias oriented fabric held on two sides, with edge pullout from underneath the clamps The second case consists of a single layer of fabric held at the four corners, with no edge pullout. Both cases exhibit yarn ejection from the free sides.

In spite of this limitation, experimental testing of fabrics without backing is preferred from a research-oriented perspective in order to understand the impact physics before standards-based testing such as the NIJ standards with backing are employed, which is more of an end-application-oriented approach.

Previously, the sources of impact performance variability discussed were limited to the material properties of the fabric such as tensile strength. However there are other sources of variability that need to be considered. These arise from sources such as the gas gun, backing material, and ordnance such as bullet, casing, and powder. The location of the shot is also important as it contributes to the variability. It is usually impossible to ensure that every shot is at the dead center of the fabric. For the case of small or sharp projectiles and loosely woven fabrics, impacting either at the cross-over of two perpendicular yarns, or in the space between two yarns also affects the mode of deformation and consequently the impact performance. In the latter case, there is increased projectile-fabric friction and the projectile may even force the yarns apart and push its way through the fabric which is detrimental to impact performance. In fact, during both our experimental and numerical impact testing of fabrics held on two sides without backing, cases have been observed wherein the central or principal unclamped yarns have been completely ejected from the fabric which happens under certain conditions when the projectile impact occurs exactly at the central yarn cross-over. Another source of variability is the uneven fabric slippage from underneath the clamping grips.

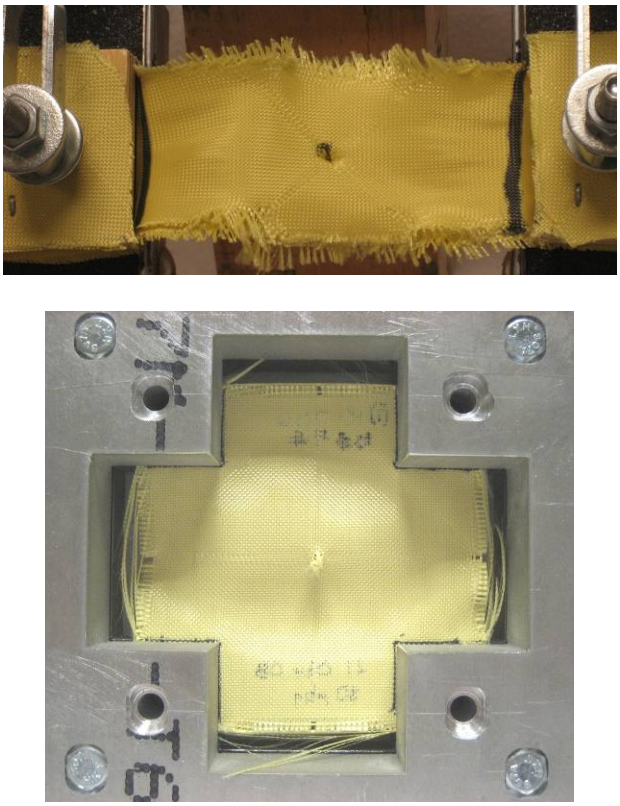

Figure 7. Experimental impact testing of Kevlar S706 fabrics (top) bias orientation held on two sides showing edge pullout (bottom) normal orientation held at four corners showing no edge pullout

As seen in an earlier section, greater weaving degradations result in weaker warp yarns. Also, warp yarns possess greater undulations or crimp compared to fill yarns, implying they take slightly longer than the fill yarns to straighten out and elongate thereby developing tension stresses under impact. However when clamping fabric targets on four sides, some amount of in-plane pretension is applied to the fabric to remove slack. This may serve to balance the crimp in the warp yarns with the fill yarns. In such a case, it is apparent that the warp yarns would fail before the fill yarns. However the smaller this pretension or greater the slack, it is no longer clear which yarn would fail earlier since the warp yarns are weaker but take longer to elongate and develop the same tension as the fill yarns since they have greater undulations. In the case of fabrics clamped on two sides, then depending on whether the warp or fill yarns are clamped would also have an effect. If only the fill yarns are clamped under tension, then the extent of undulations of the warp yarns would further increase. If the warp yarns are held under tension, then the crimp between both yarns would tend to balance out. However in the case of when only two fabric sides are clamped, the gripped yarns develop much higher tensions than the ungripped yarns. Again, depending on the relative extents of weaving damages and pretension, it is unclear which yarn, and how soon, it will fail under impact. Consequently, the pretension applied to the fabrics during clamping will also statistically affect the impact performance. This phenomenon however is different from the known deterministic effect that pre-tension has on the fabric performance,

where the tighter a fabric is clamped, the easier it is for a projectile to penetrate through the fabric.

These sources of variability and uncertainty must be factored in when interpreting experimental results, comparing results with numerical simulations, as well as comparing results from external testing agencies and the literature that adopt different in-house standards and approaches. Efforts are currently underway by us to develop a more reliable test fixture and clamping procedure for the experimental impact testing of gripped fabrics without backing, which will result in minimal fabric slippage, an even mode of fabric deformation without excessive creasing, and without excessive yarn ejection from the sides of the ungripped fabric that leads to loss of material during the test.

The proposed experimental test matrix will initially use 0.22 caliber smooth steel ball bearing projectiles against Kevlar S706 fabric targets ranging in size from a few square inches to the larger 10 in. by 10 in. fabric panels, both with single and multiple fabric plies. Later, projectiles with varying shapes and trajectories will be used. The DIC technique will be used to record strains and deformations, while velocity screens will be used to measure the residual projectile velocity. High speed cameras will record instantaneous deflections, the growth of the pyramidal deformations, as well as the instantaneous projectile velocity. The residual velocities will then be used to compare against those predicted numerically while factoring in all the uncertainties mentioned earlier. Finally the validity and applicability of the propose framework to computationally assess the statistical fabric impact performance can be studied.

6. FINITE ELEMENT MODELING OF PLAIN WEAVE FABRICS

This section outlines the setup of the fabric finite element models used in the probabilistic simulations. The fabric architecture under consideration is the Kevlar S706 fabric which is a balanced plain weave fabric comprised of 600 denier Kevlar KM2 yarns with 34 yarns per inch the warp and fill directions and an areal density of 180 g/m^2.The first step is to obtain the geometric dimensional data of the fabric architecture. This involves the cross sectional shape of the yarn and centerline

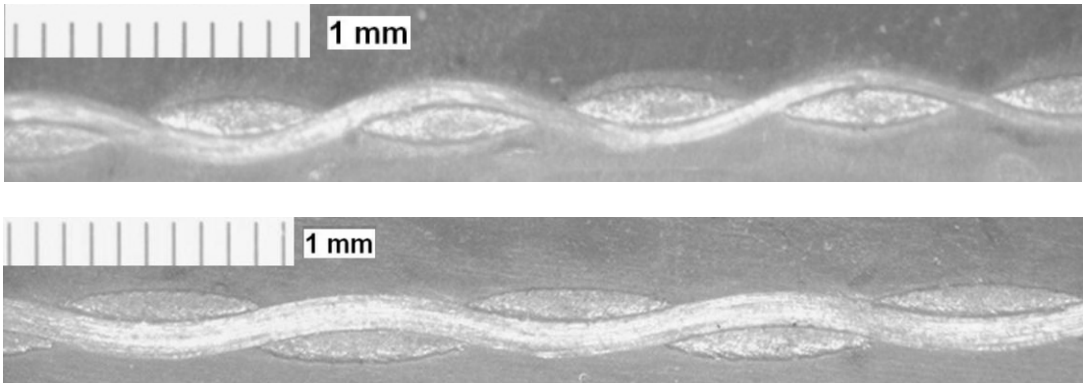

Figure 8. Micrographs of the Kevlar S706 fabric (top) warp trajectory with fill cross sections (bottom) fill trajectory with warp cross sections

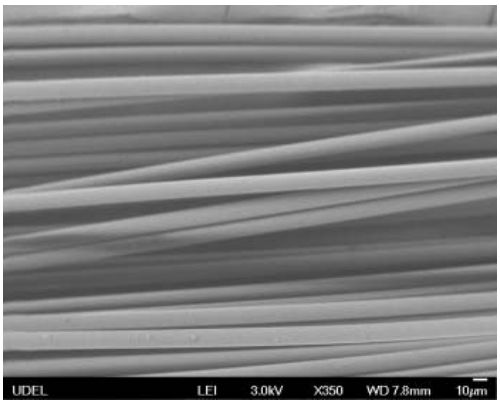

Figure 9. SEM image of filaments within the 600 denier Kevlar KM2 yarn

trajectory. Small strips of the fabric are impregnated in epoxy resin and polished to obtain micrographs. Figure (8) displays two micrographs of the yarn cross sections and trajectories as seen from the warp and fill directions. Clearly the warp yarn has a greater degree of crimp or undulations compare to the fill yarn. Figure (9) is an SEM image that shows the filaments within the yarn, taken at a magnification of 350X. Each filament has an approximate diameter of 12 microns.

From these micrographs, the yarn width, span, and thickness are measured. There are two techniques to determine the centerline trajectory. The first is to plot a series of points along the undulating centerline and record the coordinates. Then curve-fitting software is used to choose the best fit function. Another method is to mathematically derive a function based on the geometrical parameters that describe the architecture, in this case, the yarn thickness and yarn span. For a plain weave fabric the periodic cosine or sine functions work well. The warp and fill yarn trajectories can therefore be defined by

$$y = \frac{thickness}{2}\cos\left(\frac{\pi x}{span}\right) \tag{12}$$

where the ***y*** coordinate is in the thickness direction and the ***x*** coordinate is along the yarn length. However it must be noted that while these micrographs were created using fabric strips with no pretension, if the fabric FE model is to exactly represent the undulations at the time of impact when a clamped fabric with pretension is used, then either the micrographs need to be prepared with the same level of pretension that is used in the clamped fabric, or the pretension should be initially applied during the simulation to the fabric FE model.

Next, the level of detail in the model needs to be chosen. There are two possibilities while modeling the fabric with an explicit architecture that does not utilize the membrane type assumption: (*i*) filament-level (*ii*) yarn-level. In the former case, each filament within the yarn is explicitly modeled using 1-d (beam) elements. In the latter case, the yarn is assumed to be homogenous continuum. This homogenization neglects the filament level architecture. The yarn is modeled using 2-d (shell) or 3-d (brick) elements. The former case requires a greater computational infrastructure. Further, both cases have a far greater computational requirements compared to membrane-type fabric models. However new multi-scale

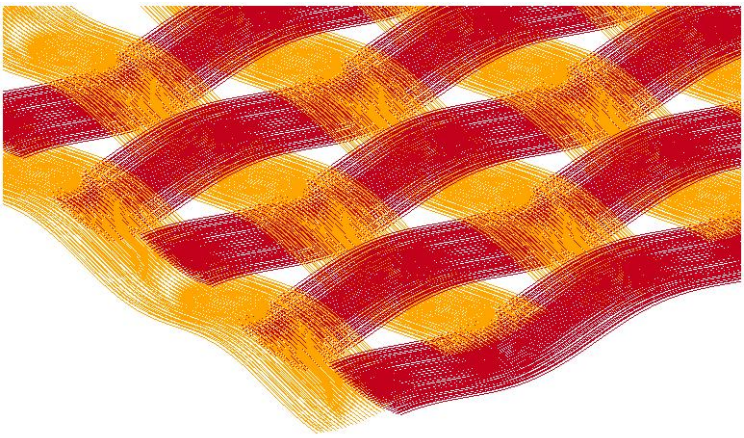

Figure 10. FE model of plain weave fabric using a filament level architecture

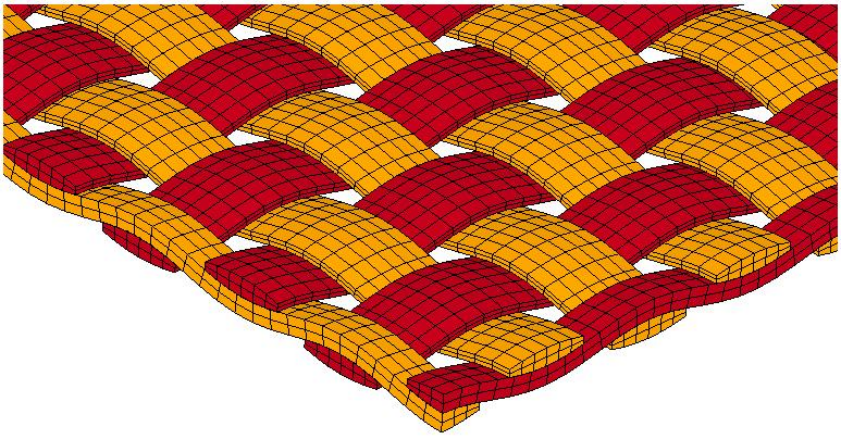

Figure 11. FE model of plain weave fabric using a yarn level architecture

modeling techniques are emerging that balance simulation accuracy with computational requirements by combining 1-d, 2-d, and 3-d elements within the same fabric model. One example is the Hybrid Element Analysis (HEA) approach by Nilakantan et al. [11-12] wherein a detailed modeling resolution is used at the impact zone and a low modeling resolution is used at far field regions. Figure (10) displays a plain weave fabric model with a filament level architecture using beam elements. Figure (11) displays the equivalent model with a yarn level architecture using solid elements. Both fabric models are created using the software DYNAFAB® [13].

When assigning material properties to the homogenized yarn, care must be taken in scaling the tensile modulus and density by the filament volume fraction. Thus the equivalent material density of the homogenized yarn will be less than that of the filament. This is necessary so that the areal density of the FE fabric model matches that of the actual fabric. Since both the tensile modulus and density are scaled down by the same amount, the longitudinal strain wave velocity remains unchanged, which is also an important requirement for high rate dynamic impact events that are governed by wave propagations and interactions. In a deterministic

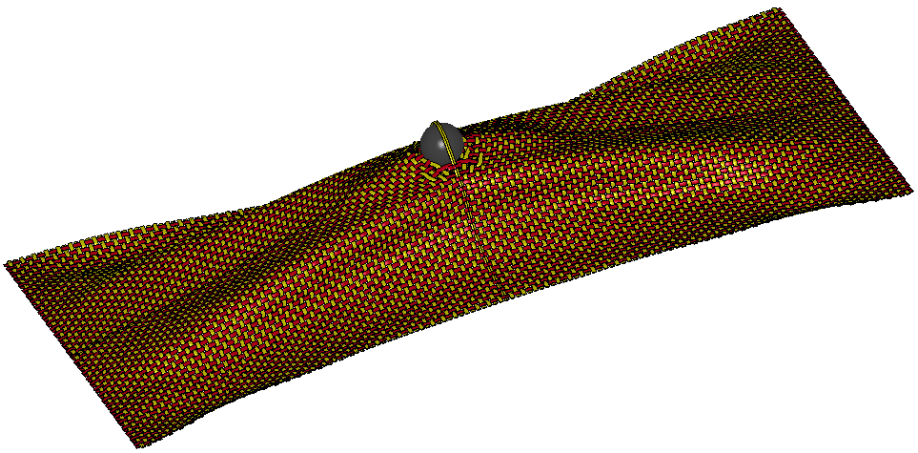

Figure 12. Snapshot from a sample deterministic impact simulation of a Kevlar S706 fabric by a spherical projectile

approach, this would be the last step before running the simulation. Figure (12) displays a snapshot from a sample deterministic impact simulation where a 0.63 gm rigid spherical projectile of diameter 5.55 mm impacts a 4 in. x 2 in. Kevlar S706 fabric at the center. The fabric is modeled using a yarn level architecture and is gripped on the two shorter sides. The free sides get pulled inwards. The central fill yarn that is unclamped begins to get pulled out from the fabric. Figure (13) displays a 4 in. x 4 in. Kevlar fabric target after being experimentally impacted using a similar projectile.

For a probabilistic simulation however, there is one final step which is the most important; and that is mapping on the experimental yarn strength distribution onto the FE model.

7. MAPPING THE STRENGTH DISTRIBUTION ONTO A FABRIC FE MODEL WITH FILAMENT LEVEL ARCHITECTURE

In this approach, each filament in the warp and fill yarns are assigned to unique strengths that follow the statistical distributions used to characterize the experimental data. Both warp and fill filaments would have separate distributions. Further depending on the length of the yarns in the fabric model, the filament strengths would be scaled using the length scale formulation outlined in Equations (10) and (11). Currently such experimental data for the strength distribution of filaments extracted separately from warp and fill yarns is unavailable. Further such experimental testing is also a challenging task since creating filament specimens of gage lengths more than a few inches is difficult because of the difficulty in handling monofilaments. Also the maximum gage length is limited by the micro tensile testing machine. However experimental data of the filament strength distribution for filaments of a single gage length extracted from a spooled yarn are available, from Ref. [1]. In spite of these challenges, such a probabilistic modeling approach is very useful because the effect of filament twist, filament-filament frictional interactions, as well as filament load sharing can be investigated. The load sharing is an important phenomenon as broken monofilaments can still carry loads because

of frictional interactions with neighboring filaments. A realistic progressive type of yarn failure will be obtained with this approach.

8. MAPPING THE STRENGTH DISTRIBUTION ONTO A FABRIC FE MODEL WITH YARN LEVEL ARCHITECTURE

In this approach, each homogenized warp and fill yarn will be assigned to unique strengths in a similar manner. The statistical strength distributions such as those displayed in Figures (3) and (4) will be mapped onto the yarns. To verify that the mapping has been performed correctly, a histogram of all assigned strengths in the fabric FE model must recreate the CDF distribution used to fit the MR data. Details of early attempts at the mapping process are available from Nilakantan et al. [14]. Figure (14) displays a fabric FE model where each yarn has been assigned to a unique strength. The color map displays the various strengths assigned to each yarn. In this approach, it is assumed that the yarn has the same strength along its entire length. For a high rate impact event where yarn failure predominantly occurs underneath the impacting projectile, this is a valid assumption. Consequently the region of interest where the mapped strengths play a role are limited to a few projectile diameters around the impact region. This is in contrast to quasi static events wherein yarn failure may occur at any point along the length, depending on the location of the critical defects in each filament.

9. DISCUSSION ON RUNNING MONTE CARLO IMPACT SIMULATIONS

Once the probabilistic fabric FE model has been set up as outlined in earlier sections, multiple runs of the simulation are conducted, and with each run, the residual projectile velocity is recorded, for a given impact velocity. With each run, the mapped strength distribution of the FE model would vary. There are many

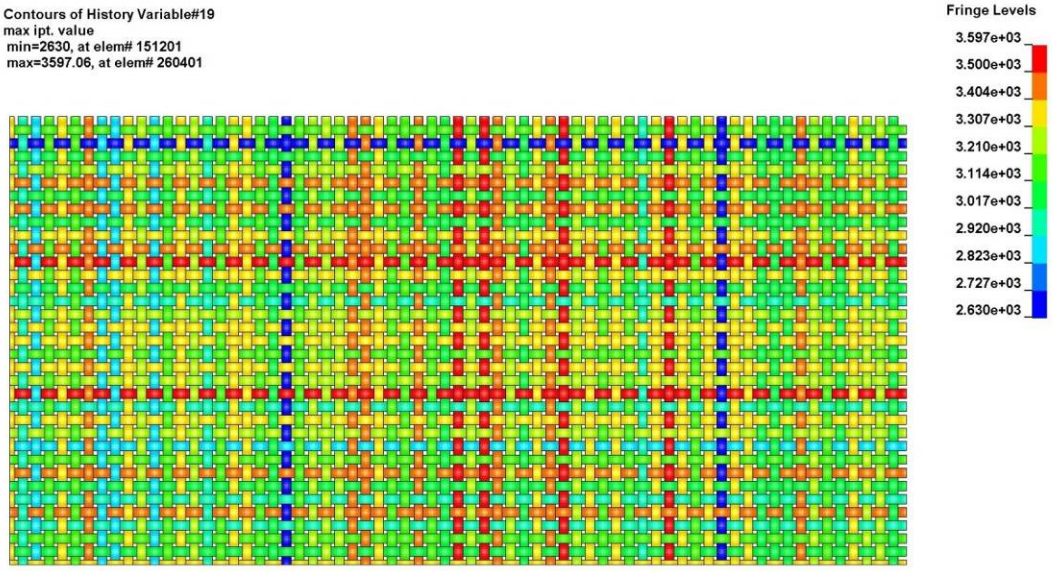

Figure 14. Fabric FE model showing contours of assigned yarn strength [14]

statistical approaches outlined in the literature on how to estimate the V_{50} velocity from a given velocity data set, as well as reports on how to perform the experimental testing in such a way as to minimize the number of shots required to estimate the V_{50} velocity. Newer approaches outline techniques to obtain the entire V_0-V_{100} probabilistic curve. One example is of Billon [15] who outlines a direct method for calculating the V_0 velocity. Such statistical work is currently beyond the scope of this paper. However the same techniques used experimentally can be directly applied to the simulation environment to guide the Monte Carlo process and eventually assess the V_0-V_{100} values.

All of the experimental strength data presented in this paper was obtained through quasistatic tensile testing at a rate of 0.5 min^{-1}. However materials such as aramids and ultra-high molecular weight polyethylenes (UHMEPE) display strain rate sensitivity with an increase in modulus and strength at higher rates. Hence it would be ideal to obtain similar experimental data at high rates as well. However there are experimental limitations on both the maximum strain rate and sample size that can be tested. For example on a split Hopkinson bar, only small filament bundles of a few millimeter length can be testing in a high rate tensile test. Consequently testing yarns with gage lengths of many inches is not possible. However by suitably altering the statistical distribution parameters using reasonable estimates or even in a parametric manner, in the case of the 3-parameter Weibull distribution they would be $\boldsymbol{\sigma_0}$, $\boldsymbol{m}$, and $\boldsymbol{x}$, the effect of strain rate could be reasonably simulated. Thus by arbitrarily or parametrically varying the statistical distribution parameters and studying their effect on the impact performance, other phenomenon could be studied too. One example would be to assess the effect of different extents of weaving damages, especially if only the strengths of the spooled material or control sample are experimentally known. Thus the impact performance of new and hybrid materials which have not yet been woven into fabrics could be studied using this probabilistic approach. This will be dealt with in future work.

10. PROBABILISTIC FRAMEWORK: FROM START TO FINISH

This section provides a flow chart of the overall framework, see Figure (15), necessary to computationally assess the statistical impact performance of woven fabrics. As mentioned earlier, this paper deals with only a part of the overall framework. Future work will deal with subsequent stages of the framework.

11. CONCLUSION

An experimental data set of the quasistatic tensile strengths of 600 denier Kevlar KM2 yarns obtained from a spool and extracted from greige and scoured Kevlar S706 fabrics has been presented. Statistical techniques using the G-Gamma and 3-parameter Weibull distributions were employed to characterize the experimental data. A new length scale formulation was presented to predict the CDF of any gage length using a single known gage length, providing the gage lengths extrapolated to lie within a close range of the gage length extrapolated from. Weaving degradations led to the yarns extracted from the fabric having lower strength distributions

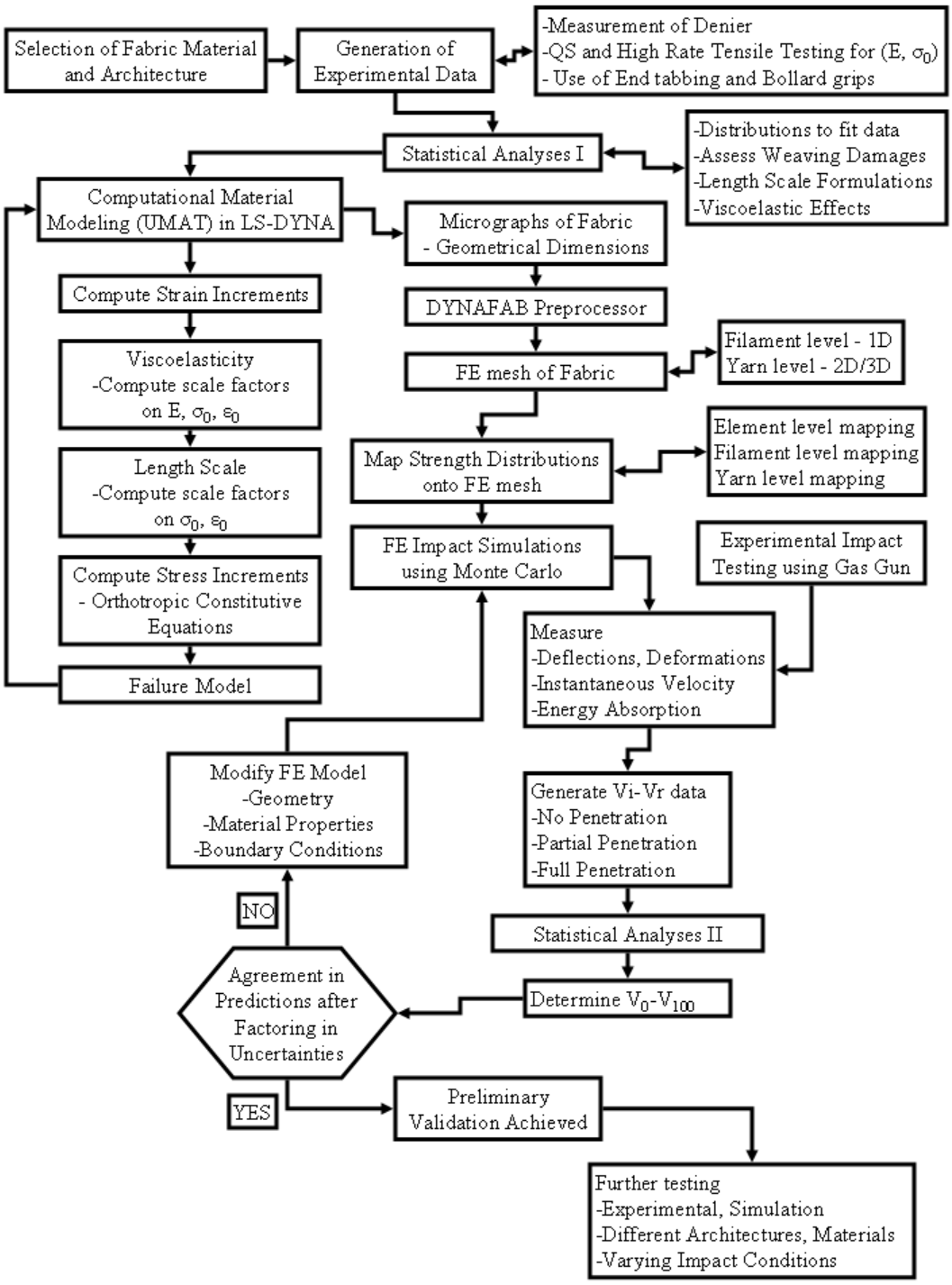

Figure 15. Flowchart of the overall framework

compared to the yarns from the spool. Warp yarns suffered greater strength degradations compared to fill yarns. The process of scouring further degrades the strength. At higher gage lengths, the strength distributions shifted to lower strengths. This is associated with the greater probability of locating a critical defect.

The setting up of the finite element mesh of the fabric using geometric dimensional data from micrographs was outlined. Modeling a fabric with a filament level architecture provides the ability to study filament-filament interactions and load sharing mechanisms which lend further insight into the impact physics over analyses that utilize a yarn level architecture. However this approach has increased computational requirements which could potentially limit the size of the fabric target simulated. Hence multi-scale modeling techniques need to be employed.

A framework for the entire probabilistic simulation approach to the modeling the impact of woven fabrics was presented. This included setting up the fabric FE model and mapping the statistical strength distributions onto the FE mesh. Uncertainties associated with experimental impact testing were outlined to enable a proper comparison between experimental and numerical simulation results. In order to reduce the fabric slippage from underneath the clamps during experimental impact testing of fabrics, new robust grip designs are required, for which work is currently underway. The next stage of experimental impact testing will involve the shooting of 0.22 caliber smooth steel ball bearing projectiles against small single-layered Kevlar S706 fabric targets. Statistical techniques will be used to develop the V_0-V_{100} curve. Next, Monte Carlo type FE simulations will be conducted using the framework outlined herein. Results will be compared in order to assess the validity of this approach.

It is envisioned that eventually a reliable and predictive computational framework will be established wherein the probabilistic impact performance of fabrics comprised of any material and architecture, and under various impact conditions can be studied thereby reducing the dependence on, and time and cost associated with large scale experimental impact testing meant to achieve the same purpose.

12. ACKNOWLEDGEMENTS

The financial support of the US Army Research Laboratory (ARL) at the Aberdeen Proving Grounds, MD, USA, and the Center for Composite Materials (CCM) at the University of Delaware, DE, USA is gratefully acknowledged. Dr. Joseph Deitzel (CCM Scientist) is acknowledged for many helpful technical discussions. Dr. Eric Wetzel (ARL) and Mr. Richard Merrill (ARL) are acknowledged for their assistance with the experimental impact testing of the fabrics.

13. REFERENCES

[1] Leal, A.A., Deitzel, J.M., and Gillespie, J.W. Jr., "Assessment of compressive properties of high performance organic fibers," *Composites Science and Technology*, Vol. 67, 2007, pp. 2786–2794.

[2] Leal, A.A., Deitzel, J.M., and Gillespie, J.W. Jr., "Compressive Strength Analysis for High Performance Fibers with Different Modulus in Tension and Compression," *Journal of Composite Materials*, Vol. 43, 2009, pp. 661-674.

[3] Abu-Obaid, A., Andersen, S.M., Gillespie, J.W. Jr., Dickenson, B., Watson, A., Chapman, G., and Coffelt, R.A., "Effects of weaving on S-2 glass tensile strength distributions," *TEXCOMP 9, University of Delaware, Newark, DE, USA*, October 13-15, 2008.

[4] Abu-Obaid, A., Andersen, S.M., Gillespie, J.W. Jr., Dickenson, B., Watson, A., Chapman, G., and Coffelt, R.A., "Effects of 3D weaving on tensile strength retention of Z-tows," *Second World*

Conference on 3D Fabrics and their Applications, Greenville, South Carolina, USA, April 6-7, 2009.
[5] Goda, K., and Fukunaga, H., "The evaluation of the strength distribution of silicon carbide and alumina fibers by a multi-modal Weibull distribution," *Journal of Materials Science,* Vol. 21, 1986, pp. 4475-4480.
[6] Wang, Y., and Xia, Y., "Experimental and theoretical study on the strain rate and temperature dependence of mechanical behavior of Kevlar fiber," *Composites, Part A,* Vol. 30, 1999, pp. 1251-1257.
[7] Phoenix, S.L., and Smith, R.L., "A comparison of probabilistic techniques for the strength of fibrous materials under local load-sharing among fibers," *International Journal of Solids and Structures,* Vol. 19, 1983, pp. 479-496.
[8] "Reliasoft Weibull++® Technical Documentation," *Reliasoft*, ©Copyright 2009, On the Web: www.reliasoft.com
[9] Wu, H.F., and Netravali, A.N., "Weibull analysis of strength-length relationships in single Nicalon SiC fibres," *Journal of Materials Science*, Vol. 27, 1992, pp. 3318-3324.
[10] Phoenix, S. L., Schwartz, and Robinson, H. H., IV, "Statistics for the Strength and Lifetime in Creep-Rupture of Model Carbon/Epoxy Composites," *Composites Science and Technology*, Vol. 32, 1988, pp. 81-120.
[11] Nilakantan, G., Keefe, M., Gillespie, J.W. Jr., and Bogetti, T.A., "Novel multi-scale modeling of woven fabrics for use in impact studies," *10th International LS-DYNA Users Conference, Dearborn, MI, USA,* June 8-10, 2008.
[12] Nilakantan, G., Keefe, M., Gillespie, J.W. Jr., and Bogetti, T.A., "Simulating the impact of multi-layer fabric targets using a multi-scale model and the finite element method," *TEXCOMP 9, University of Delaware, Newark, DE, USA*, October 13-15, 2008.
[13] Nilakantan, G., "DYNAFAB® User Manual," *Nilakantan Composites*, ©Copyright 2009, On the Web: www.nicomposites.com
[14] Nilakantan, G., Keefe, M., Gillespie, J.W. Jr., and Bogetti, T.A., "Modeling the material and failure response of continuous filament fabrics for use in impact applications", *TEXCOMP 9, University of Delaware, Newark, DE, USA*, October 13-15, 2008.
[15] Billon, H.H., "N new method for calculating the critical penetration velocity (V_0)," *DSTO-TN-0791*, December 2007.